

Airfoil noise measurements at various angles of attack and low Reynolds number

Elias J. G. Arcondoulis, Con J. Doolan and Anthony C. Zander

School of Mechanical Engineering, University of Adelaide, Adelaide, Australia

ABSTRACT

Airfoils produce tonal noise when operated at low-to-moderate Reynolds number. It is particularly annoying to the human ear and is problematic for the design of fans, compressors, helicopter rotors and unmanned air vehicles. Despite recent advances in the understanding of this phenomenon, there are still many unresolved aspects regarding the aerodynamic source generation mechanism. In this paper, the trailing edge noise characteristics of a NACA0012 airfoil at low Reynolds numbers (50,000 to 175,000) are presented. Experimental measurements show that the noise consists of a multitude of tones centered about a broadband component. Such noise spectra are not observed at higher Reynolds numbers. The effect of angle of attack and Reynolds number will be discussed along with possible source generation mechanisms.

INTRODUCTION

To date, there have been many investigations into the causes and mechanisms responsible for the trailing edge noise of airfoils in low Reynolds number flow regimes. Well known experimental studies include Paterson et al. 1973, Tam 1974, Arbey et al. 1983, Nash et al. 1999, Kingan & Pearse 2009 and Chong & Joseph 2009. Numerically based analyses include Wang 1998, Desquesnes et al. 2007 and Sandberg et al. 2008.

Following the explanation of Desquesnes et al. 2007, a laminar boundary layer is formed near the leading edge of an airfoil under steady flow. This continues along the airfoil chord until boundary layer separation occurs, leading to an unstable shear layer with Tollmien-Schlichting (TS) instability waves. The hydrodynamic fluctuations interact with the trailing edge, forming a dipole acoustic source. The acoustic waves then travel back along the airfoil chord, supposedly generating an acoustic feedback loop. This is depicted in Figure 1.

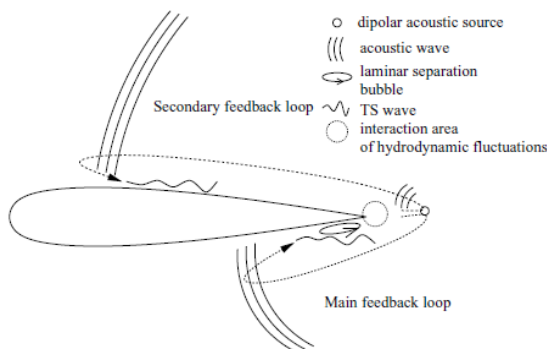


Figure 1: Scheme of the Tonal Noise Mechanism (Desquesnes et al. 2007).

It is believed that the tonal noise phenomenon is caused by a feedback mechanism, yet in each study mentioned prior, there are differing explanations. Arbey et al (1983) and Chong and Joseph (2009) provide some consensus suggesting that a feedback mechanism exists due to an unstable boundary layer. However, Nakano et al. (2006) suggested that the tonal noise is generated from the periodic vortex structure

near the trailing edge on the pressure surface of the airfoil. Nash et al. (1999) suggest that the growth of TS instability waves are amplified by inflectional profiles in the separating laminar shear layer on the pressure surface of the airfoil. Kingan & Pearse (2009) brought the work of Arbey (1983) and Nash et al. (1999) together, creating a theoretical laminar boundary layer instability noise model to suit their data. This aside, there is no general consensus in the acoustic community for this trailing edge noise mechanism, nor have sufficient experimental measurements been performed to confirm or deny the various proposed mechanisms.

This paper details an experimental investigation of trailing edge noise for a NACA0012 airfoil at low Reynolds number. The experiments were conducted in the Anechoic Wind Tunnel (AWT) in the Holden Lab of the University of Adelaide. The investigated airfoil has a chord length of 67mm and was operated under Reynolds numbers (Re) 50,000 to 175,000.

EXPERIMENTAL FACILITY

The AWT is a low-speed wind tunnel, designed for scale model testing, with a total room size of approximately 2m³. The walls are acoustically treated with foam wedges, to minimise sound reflection and to maximise sound absorption. The contraction outlet (test section) has a working area of 75mm (height) x 275mm (width). The AWT facility including the contraction and the airfoil housing are shown in Figure 2.

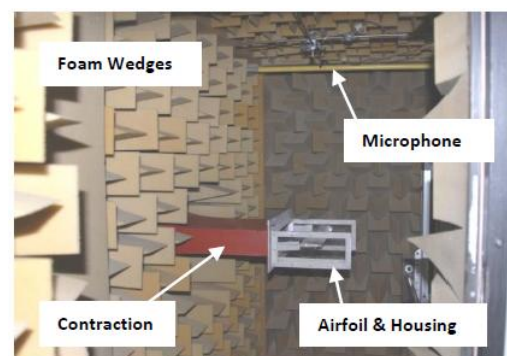


Figure 2: View of the AWT Facility.

The fan driving the airflow in the AWT is governed by a speed controller which limits its RPM to 50Hz, corresponding to a test section speed (U) of 40m/s. Note that this restricts the airfoil span which can be used as well as the Reynolds numbers that can be investigated.

Noise spectra were acquired using single microphone measurements. The microphone is a sub-miniature condenser microphone manufactured by Lectret (Model 1207), possessing a uniform frequency response from 30Hz to 15kHz, which is suitable for this application. The microphones were calibrated prior to installation.

A NACA0012 airfoil section was used for all of the experiments presented in this paper. The chord is 67mm, with a span of 275mm. The airfoil is secured in its housing 50mm from the plane of the contraction outlet using a rod protruding through the airfoil along its axis of maximum thickness. This rod is then fastened to the housing at both ends of the airfoil span, which is directly attached to the contraction, as shown in Figure 3.

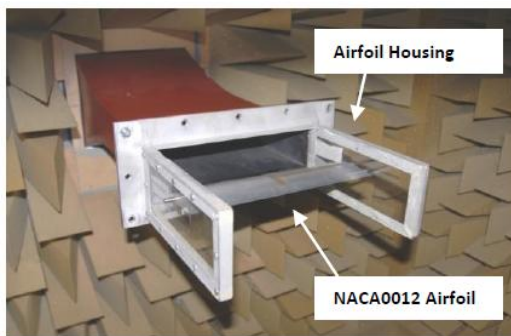


Figure 3: AWT Airfoil Testing Configuration.

Due to the height of the test section, it was investigated whether the airfoil thickness would significantly impact the flow exiting the contraction. The jet height is 75mm and the maximum measured thickness of the airfoil is 8mm. Thus, the blockage of airflow due to the airfoil is less than 11%, which was deemed acceptable.

Shear Layer Refraction

The amount of refraction experienced by an acoustic wave propagating through a shear layer is dependent upon the Mach number of the jet flow, the width of the jet, and the distance and angle from which the acoustic source is located relative to the observer (i.e. microphone) (Amiet 1977). Corrections must be made to account for the amount an acoustic wave is refracted through the shear layer of the test section. This determines where a microphone should be placed to receive accurate noise measurements from the trailing edge.

As the primary concern of this paper is to detail the nature of the trailing edge noise, rather than the specific magnitudes and phases of the acoustic waves, the microphone was placed at a location corresponding to the average geometric distance between where the shear layer would be refracted in the case of the Reynolds number being 50,000 and 175,000. While it is assumed that the directionality response of the microphone is uniform over a ±10° range, the placement of the microphone is acceptable on the basis that for each Reynolds number case, the spectra measured by the microphone will not be restricted due to the directionality of the incoming acoustic waves.

Figure 4 is a schematic diagram detailing the geometry and parameters required to compensate for shear layer refraction (adapted from Amiet (1977)). The vertical distance of the acoustic source (being the trailing edge) is 650mm (R_m) and half the width of the jet is 37.5mm (R_t).

Equation 1 was derived from Amiet’s equations for shear layer refraction in an open jet (1977). There existed three equations with three unknowns, yet an explicit solution could not be attained via rearrangement. It was assumed that the microphone was placed directly above the noise source and that the noise radiated in the same direction (θ_m = 90°). These equations were then combined to create a modified equation in terms of only one variable, θ’:

$$\frac{\cos(\theta') - M_0}{\sin(\theta')} + \left[\left(\frac{R_m}{R_t} \right) - 1 \right] \cot \left[\cos^{-1} \left(\frac{\cos(\theta')}{1 - M_0 \cos(\theta')} \right) \right] = 0 \tag{1}$$

which may be iteratively solved for θ’.

In the case of the 67mm chord airfoil, the Reynolds number range of 50,000 to 175,000 corresponds to a Mach number (M₀) range of 0.03 (minimum) to 0.12 (maximum). Solving Equation 1 using known values for R_m, R_t, and M₀ for minimum and maximum cases, results in a total flow deviation |θ_m - θ| = 1.8° and 6.2° respectively. The average of these two angles is 4.0°.

Using trigonometry and calculating that θ₀ ≈ θ’ for θ_m = 90°, the distance the microphone should be shifted downstream of the noise source (i.e. airfoil trailing edge) is tan(3.6°) × 650mm = 45.45mm. This value was rounded to 45mm, as shown in Figure 5. Note that it is assumed that the change to R_m (i.e. 650mm increases to 651.2mm) has a negligible effect of the amount of shear layer refraction. This makes the design process much simpler, preventing further iteration processes.

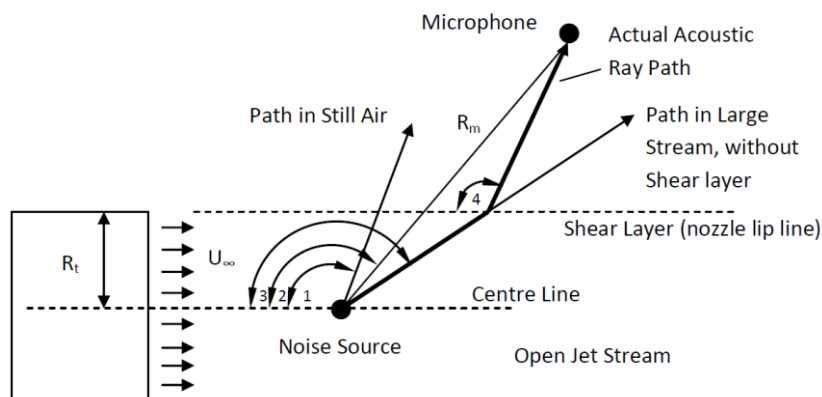


Figure 4: Shear Layer Refraction Schematic Diagram, where angle 1 is θ’, angle 2 is θ_m, angle 3 is θ’ and angle 4 is θ₀.

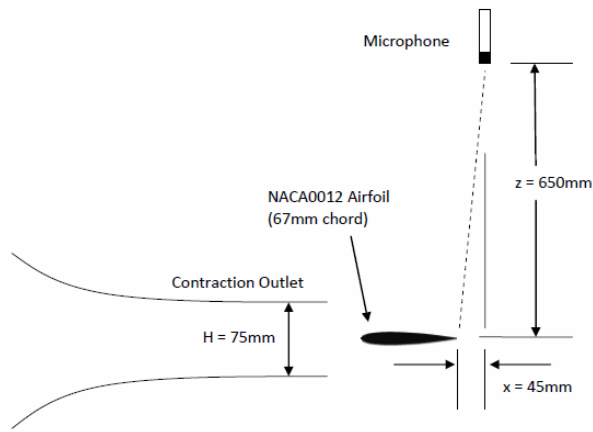


Figure 5: AWT Airfoil Testing Schematic Diagram.

Anechoic Chamber Performance

From preliminary testing, the range of frequencies measured from the airfoil section was 500 Hz to 10 kHz. It is aimed that the noise of interest will be within the anechoic range of the facility, which has a design limit of 200Hz.

A measurement of background noise with no airflow in the AWT was recorded. The results of this measurement are provided in Figure 6. Note that all plots herein are provided intentionally for frequencies from 100Hz to 10kHz and magnitudes 0dB to 100dB, with reference 20×10^{-6} Pa.

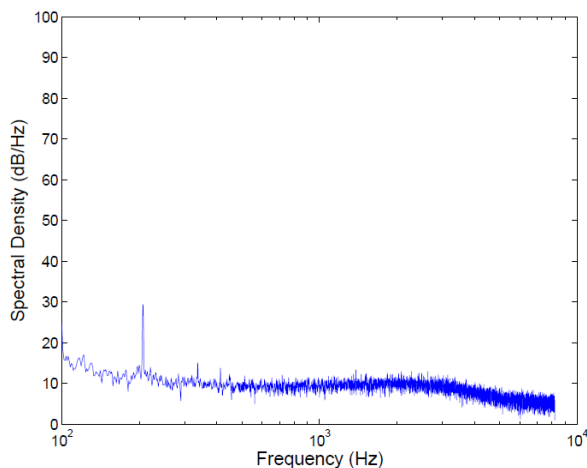


Figure 6: Background AWT Noise Spectra, no airflow.

There exists a peak at approximately 200Hz, which is most likely due to either electrical lighting noise or “humming” from computer screens. Note that despite its narrow band behaviour, it still only has magnitude of 30dB. This figure also shows that the microphone’s self-noise is relatively uniform and small.

The AWT was then operated at all fan speeds (without the test article or airfoil) equivalent to the experimentally chosen Reynolds numbers to acquire the background spectra. It can be seen by comparing Figure 6 with the following Figure 7 that the noise due to airflow of 11.3m/s in the AWT (corresponding to an airfoil $Re = 50,000$ if a 67mm airfoil were in place) results in a very small increase in background noise.

As the airflow velocity was increased to 33.8m/s (corresponding to a $Re = 150,000$ if a 67mm airfoil were in place), there was a marked noise increase at frequencies less than 1kHz, shown in Figure 7. Above this frequency, the background noise rises by about 10dB.

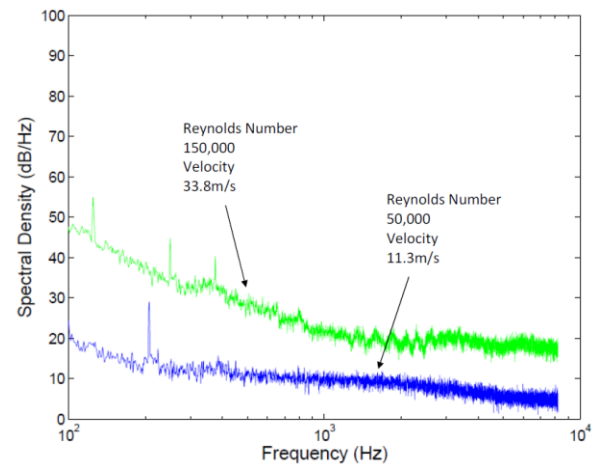


Figure 7: Background AWT Noise, $Re = 50,000$ & $150,000$, $U_{\infty} = 11.3m/s$ and $33.8m/s$ respectively.

It can be seen in Figure 7 that the background noise is approximately 35dB at 300Hz, for $Re = 150,000$. This represents the worst case background noise magnitude in the frequency range of interest, as the airfoil noise spectra of interest are greater than 300Hz (see Results and Discussion).

EXPERIMENTAL PROCEDURES

Data Acquisition

A National Instruments (NI) data card was used to obtain the microphone data. A MATLAB Data Acquisition (DAQ) interface was used to collect this data, which was then able to be further processed. Fast Fourier Transform (FFT) was used to convert the data from the time into the frequency domain, to obtain the spectral density. The microphone voltages were converted into Sound Pressure Level (SPL).

The data was acquired at a sampling frequency of 16384 Hz (2^{14} Hz) in four blocks of 1 second. The presented data is the average of the four data sets, with a frequency resolution of 1Hz. The range of frequencies covered in the noise spectra is 0Hz to 8192Hz (2^{13} Hz).

Reynolds Number

The noise spectra for the NACA0012 airfoil were taken at $Re = 50,000$ to $150,000$, in increments of 25,000. This allowed the direct comparison with other experimental and numerical investigations, such as Arbey et al. (1983) and Desquesnes et al. (2007), who investigated NACA0012 airfoils at $Re = 106,000$ and higher.

As well as the maximum allowable AWT test section speed constraining the Reynolds number range, the distinct tonal behaviour for the airfoil placed at 0° angle of attack was far less defined at $Re > 150,000$. Thus it was decided not to obtain results at any higher Reynolds numbers at 0° angle of attack.

Angle of Attack

The airfoil was placed at three geometric angles of attack during testing, 0° , 5° and 10° .

Since the AWT jet height is finite, two-dimensional correction factors were applied to determine the true effect of the airfoil angle of attack (Brooks et al. 1989). Generally the true angle of attack is much less than the geometric angle of attack of the airfoil for small jet height testing environments.

The correction factor is:

$$\alpha' = \frac{\alpha}{\zeta} \tag{2}$$

where α' is the true angle of attack, α is the geometric angle of attack, and ζ and σ are given by:

$$\zeta = (1 + 2\sigma)^2 + \sqrt{12}\sigma \tag{3}$$

$$\sigma = \left(\frac{\pi^2}{48}\right) \left(\frac{C}{H}\right)^2 \tag{4}$$

where C is the airfoil chord length (67mm) and H is the jet height at which the airfoil is placed (75mm). Note that the airfoil is placed 50mm from the contraction outlet and it is assumed that the flow jet height at the airfoil location is the same as it is inside the test section. Thus, the actual angles of attack presented in this paper are calculated as:

$$0^\circ \equiv 0^\circ \quad (\text{true})$$

$$5^\circ (\text{geometric}) \equiv 1.58^\circ \quad (\text{true})$$

$$10^\circ (\text{geometric}) \equiv 3.16^\circ \quad (\text{true})$$

Throughout the remainder of this paper, only the true angle of attack (α') will be stated.

RESULTS AND DISCUSSION

Angle of Attack: 0°

At a $Re = 50,000$, discrete tones are noted in the noise spectra, as shown in Figure 8. Note that the small peak at approximately 200Hz is most likely background noise (as discussed earlier and displayed in Figure 6). A small broadband hump has formed from approximately 200Hz to 800Hz.

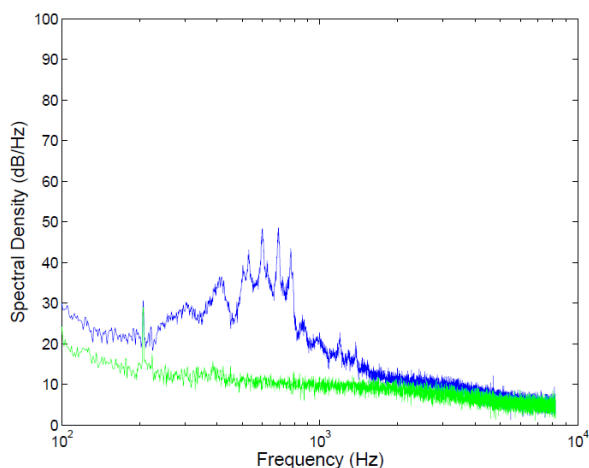


Figure 8: NACA0012 & Background Spectra, $\alpha' = 0^\circ$, $Re = 50,000$.

As the Reynolds number is increased to 75,000, changes are noticed in the noise spectra, as shown in Figure 9. These were clearly audible to the authors while standing inside the AWT during preliminary testing. The discrete tones are far more pronounced, and have increased in frequency to 900Hz to 1.5kHz. The broadband hump has widened and is located between approximately 500Hz to 2kHz. Note that at this Reynolds number, there is still very little contribution to frequencies greater than 3kHz (spectra at such frequencies are less than 20dB). These results agree with the shape of the

spectral density plot of Arbey et al. (1983). For clarity, an enlargement of Figure 9 is provided in Figure 10.

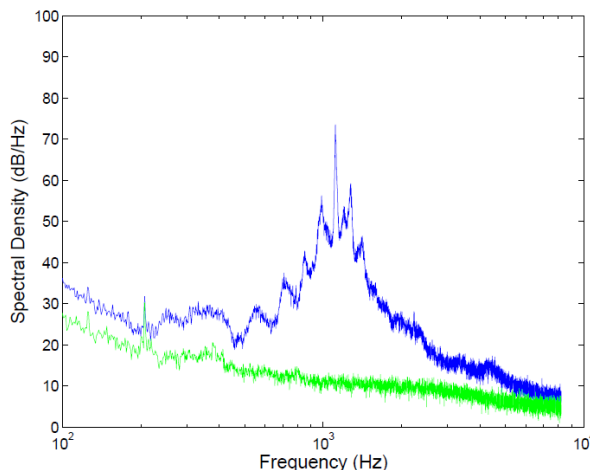


Figure 9: NACA0012 & Background Spectra, $\alpha' = 0^\circ$, $Re = 75,000$.

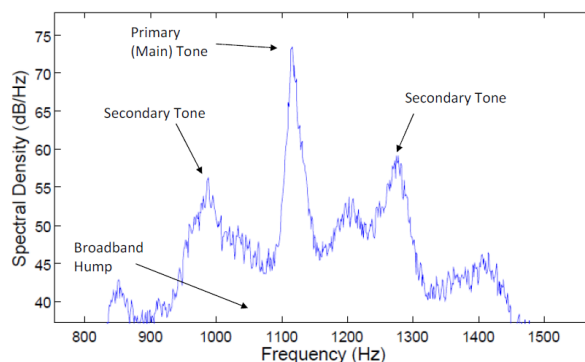


Figure 10: Enlargement of Figure 8 (linear scale) including identification of Noise Spectra features.

At $Re = 100,000$, a second broadband hump with a superimposed tone is noticed at approximately 2.5kHz, as shown in Figure 11. It is evident that the increase in airflow speed provides a contribution to the higher frequency of the airfoil noise spectra, as there is negligible noise at frequencies greater than 2kHz at $Re = 50,000$.

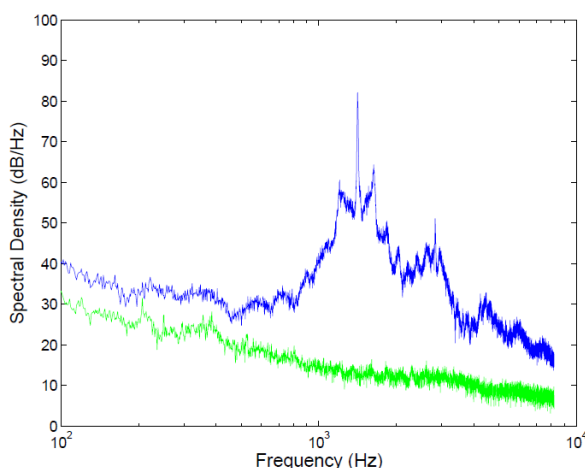


Figure 11: NACA0012 & Background Spectra, $\alpha' = 0^\circ$, $Re = 100,000$.

The Reynolds number was increased to 150,000. The result is a frequency shift of the tones to higher frequencies (shown in Figure 12). The tonal magnitudes are lower in this noise spectra plot. In addition, there is very little noise contribution at frequencies less than 1kHz. There is a broader band of higher

frequency noise than at lower Reynolds numbers, especially from 3kHz and higher.

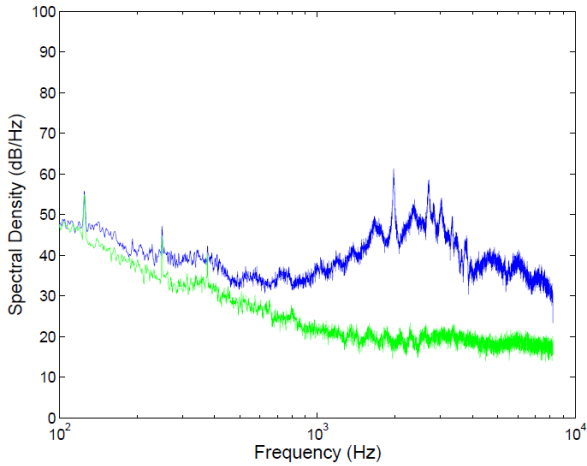


Figure 12: NACA0012 & Background Spectra, $\alpha' = 0^\circ$, $Re = 150,000$.

At $Re = 175,000$ for $\alpha' = 0^\circ$, the tonal behaviour was far less pronounced. The noise spectra were much broader without any noticeable tones. This was immediately audible during testing as the AWT fan speed increased to reach $Re = 175,000$.

Angle of Attack: 1.58°

The results for $\alpha' = 1.58^\circ$ are almost identical to $\alpha' = 0^\circ$, up to and including $Re = 125,000$. This strongly suggests that the effect of increasing α' to 1.58° is minimal, for such a Reynolds number range and airfoil profile. However, at $Re = 150,000$, the noise spectra differed. While the tonal magnitude had decreased from $Re = 100,000$ for both angles of attack, the $\alpha' = 1.58^\circ$ case still presented a much clearer, more defined primary tone (75dB compared to 62dB at $\alpha' = 0^\circ$). The noise spectra for $Re = 150,000$ are presented in Figure 13.

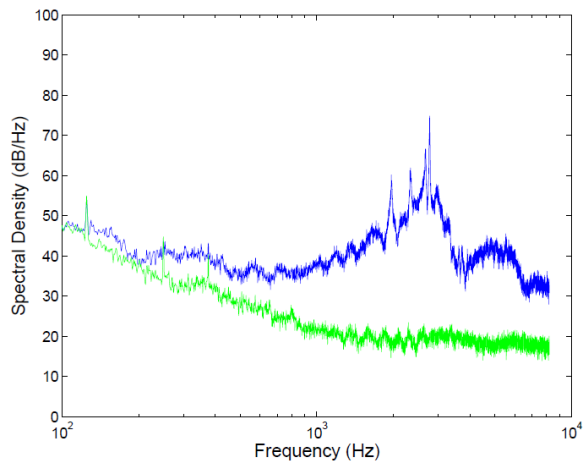


Figure 13: NACA0012 & Background Spectra, $\alpha' = 1.58^\circ$, $Re = 150,000$.

Angle of Attack: 3.16°

The results for $\alpha' = 3.16^\circ$ are very different from the 0° and 1.58° cases. For $Re = 50,000$ to $125,000$, no distinct tonal behaviour was detected. At $Re = 50,000$, the noise spectra (being the “start” of the broadband hump) barely exceeded the background noise. This is shown in Figure 14.

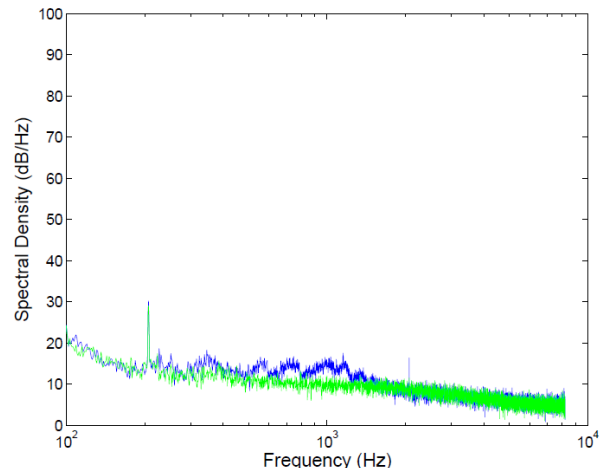


Figure 14: NACA0012 & Background Spectra, $\alpha' = 3.16^\circ$, $Re = 50,000$.

At $Re = 75,000$, the typical broadband hump centred about 1.8kHz began to form. This continued to $Re = 125,000$, where the hump became more defined, yet the presence of tones was not yet observed, as shown in Figure 15.

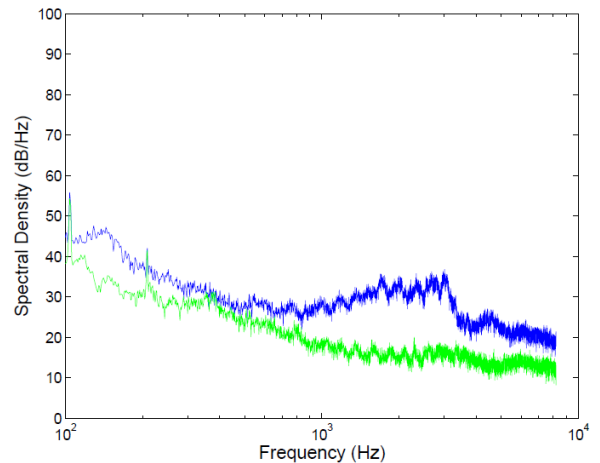


Figure 15: NACA0012 & Background Spectra, $\alpha' = 3.16^\circ$, $Re = 125,000$.

From $Re = 125,000$ to $150,000$, significant changes occurred to the noise spectra. Distinct tones were superimposed on the broadband hump, resembling the behaviour of $Re = 150,000$ for $\alpha' = 1.58^\circ$, but shifted to a higher frequency. This is shown in Figure 16.

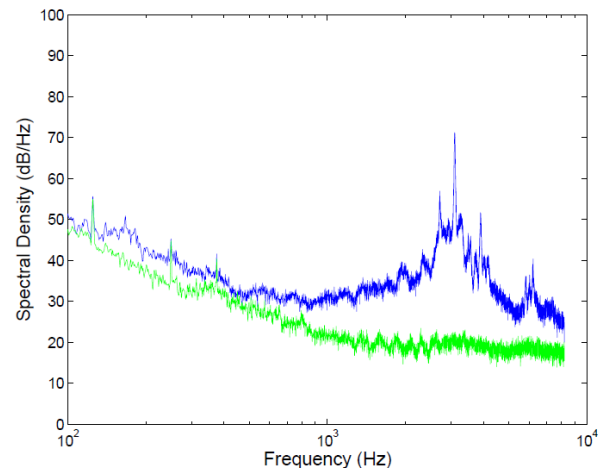


Figure 16: NACA0012 & Background Spectra, $\alpha' = 3.16^\circ$, $Re = 150,000$.

Increasing the Reynolds number to 175,000 clearly showed the presence of tones superimposed with a broader hump. This shows that the tonal behaviour continues beyond $Re = 150,000$ for this angle of attack.

Noise Magnitude

While the noise spectra in the previous sections displayed the nature of the tonal noise structures as well as the range of frequencies radiated from the airfoil trailing edge, the magnitudes of the noise spectra of various frequencies are compared for $50,000 \leq Re \leq 150,000$. This provides a different perspective to the noise behaviour as well as identifying some characteristics about the noise spectra which may not be immediately obvious by looking directly at noise spectra plots alone. Figure 17 through Figure 19 display the airfoil noise magnitude for a given frequency (1kHz, 1.5kHz and 2.5kHz) and how it varies with Reynolds number.

It can be seen in Figure 17 that the 1kHz noise is nearly identical for the $\alpha' = 0^\circ$ and 1.58° cases and shows a maximum at $Re = 75,000$. Interestingly the $\alpha' = 3.16^\circ$ case shows an approximately linear dB increase in noise with a linear increase in Reynolds number, displaying no local maximum and a generally smaller magnitude.

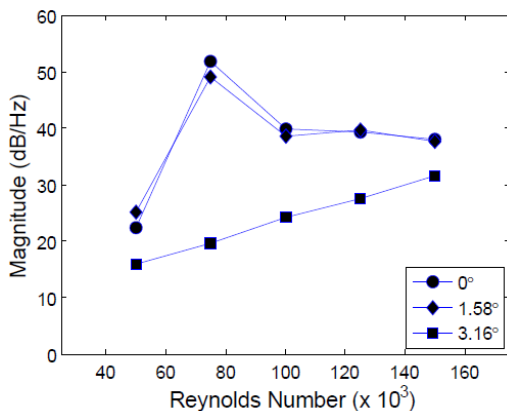


Figure 17: NACA0012 Noise Magnitudes (1kHz). The $\alpha' = 3.16^\circ$ case is fitted by $p = 0.692 \times U + 8.133$, where p is acoustic pressure (dB) and U is airflow speed (m/s).

Consistent with Figure 17, the noise magnitudes at a frequency of 1.5kHz show similar behaviour as seen in Figure 18. The maximum noise for the $\alpha' = 0^\circ$ and 1.58° cases occurs at $Re = 100,000$ and the $\alpha' = 3.16^\circ$ case again gives an approximate linear dB increase in noise and no local maximum.

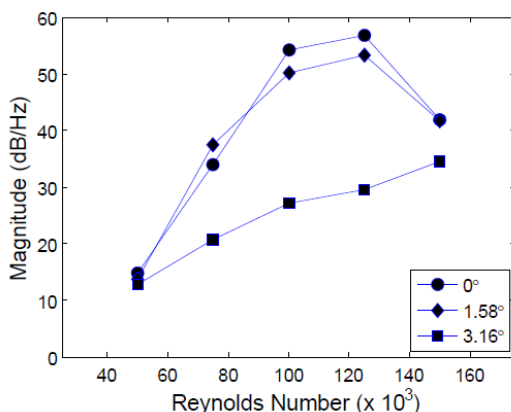


Figure 18: NACA0012 Noise Magnitudes (1.5kHz). The $\alpha' = 3.16^\circ$ case fitted by $p = 0.933 \times U + 3.921$.

Measurements at 2.5kHz provide completely different results to the lower frequency cases for $\alpha' = 0^\circ$ and 1.58° . As illustrated in Figure 19, the noise magnitudes (in dB) for all three angle of attack cases are approximately linearly increasing with Reynolds number.

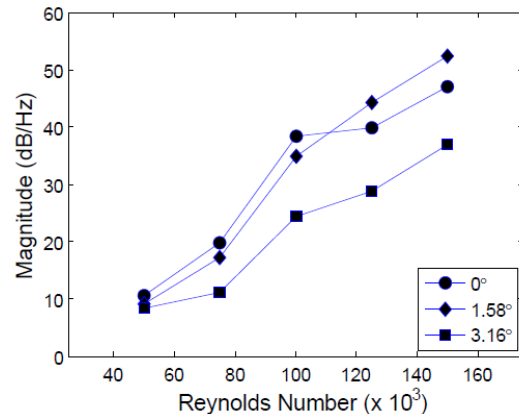


Figure 19: NACA0012 Noise Magnitudes (2.5kHz).

At frequencies greater than 2.5kHz, similar behaviour is noticed. While the noise magnitudes (in dB) did not appear to be increasing linearly with Reynolds number, there are no local maxima or identifiable features to suggest a strong influence of tonal behaviour at this frequency.

In all cases, the linear increase of noise (dB) appears consistent with expected turbulent boundary layer behaviour on the suction side of the airfoil, as observed by Sandberg et al. (2008). This generates boundary layer separation from the airfoil, thus removing the mechanism responsible for tonal noise (and causes broadband noise). At lower angles of attack, the boundary layer remains laminar and this does not occur.

Ladder Structure

As measured by Paterson et al. (1973), the primary tone of an airfoil follows a general trend given by:

$$f = \frac{0.011U^{1.5}}{\sqrt{C\nu}} \tag{5}$$

where C is the chord of the airfoil, ν is the dynamic viscosity. This equation is plotted in Figure 20.

While this curve fits the general trend of the primary tone, it does not accurately model them. For a given angle of attack, the frequencies follow a $U^{0.8}$ power law, but at a certain Reynolds number, the frequency suddenly ‘‘jumps’’, forming a new $U^{0.8}$ dependency, thus forming a ‘‘ladder structure’’. Over a range of Reynolds numbers and angles of attack, the frequency dependency eventually fits a $U^{1.5}$ curve. This is well noted for low Reynolds number trailing edge noise in many early publications, such as Arbey et al. 1983 and Nash et al. 1998.

Some of the attained results presented in this paper also follow this ladder structure phenomenon (shown in Figure 20). It may be less obvious to visualise, as compared to the other papers discussed prior. This is mainly due to the limited range of Reynolds numbers able to be tested.

At both $\alpha' = 0^\circ$ and 1.58° , the tonal frequency closely follows the $U^{0.8}$ power law. However, at $Re = 150,000$ for $\alpha' = 1.58^\circ$, the tonal frequency ‘‘jumps’’ to approximately 2.8kHz. In order to verify this data point, $Re = 175,000$ was operated at this angle of attack. While there are insufficient data points to

make a conclusive statement, it can be seen that the final two $\alpha' = 1.58^\circ$ cases represent the "next step" of the ladder structure, as predicted by Paterson et al. (1973).

The results at $\alpha' = 3.16^\circ$ do not follow the ladder structure behaviour. There are no clear defined tones for $Re \leq 150,000$. In addition, several tones were displayed at $Re = 175,000$ with similar magnitudes, making it difficult to determine the primary tone. Without being able to investigate higher Reynolds numbers, no conclusive statement can be made at this angle of attack.

Existence of Tones

While the frequency and magnitudes of tones from the trailing edge are of engineering importance, it is also important to know whether a tone will be present for a given airfoil, Reynolds number and angle of attack. Desquesnes et al. (2007) furthered the work of Paterson et al. (1973) and Nash et al. (1998) and generated plots of angle of attack against Reynolds number, identifying regions of the plot surface which exhibited tones or no tones. Their data was acquired for a NACA0012 airfoil, via computational solutions of the compressible Navier-Stokes equations.

Figure 21 displays the experimentally measured existence of tones for a NACA0012 airfoil, including the data displayed by Desquesnes et al. (2007). The data for angles 0° , 1.58° and 3.16° represent the present work by the authors, while Paterson et al. (1973) and Arbey et al. (1983) represent experimental results, and Nash et al. (1998) and Desquesnes et al. (2007) represent theoretical results. The two linear dashed lines represent Nash et al.'s (1998) tonal envelope prediction based on theoretical methods. It can be seen that for $\alpha' = 1.58^\circ$, $Re = 50,000$ and at $\alpha' = 3.16^\circ$ $Re = 100,000$ and $125,000$ there exists some discrepancy between the present work and Nash et al.'s (1998) prediction. In addition, at 0° angle of attack, Arbey et al. (1983) disagree with Nash et al.'s (1998) predicted envelope.

From Figure 21 it can be seen that for $\alpha' = 0^\circ$ the tonal range is from $Re = 50,000$ to $150,000$ and that at $Re = 175,000$, this tonal behaviour was not present. It is suggested here that the disappearance of the tone at $\alpha' = 0^\circ$ is due to transition to turbulence in the separated shear layer about the airfoil, destroying any feedback mechanism relying on laminar flow. The results for $\alpha' = 3.16^\circ$ are more difficult to explain. It is possibly due to a coupling of laminar separation and generation of TS waves. How these processes couple with any feedback mechanisms is still unknown and is future work.

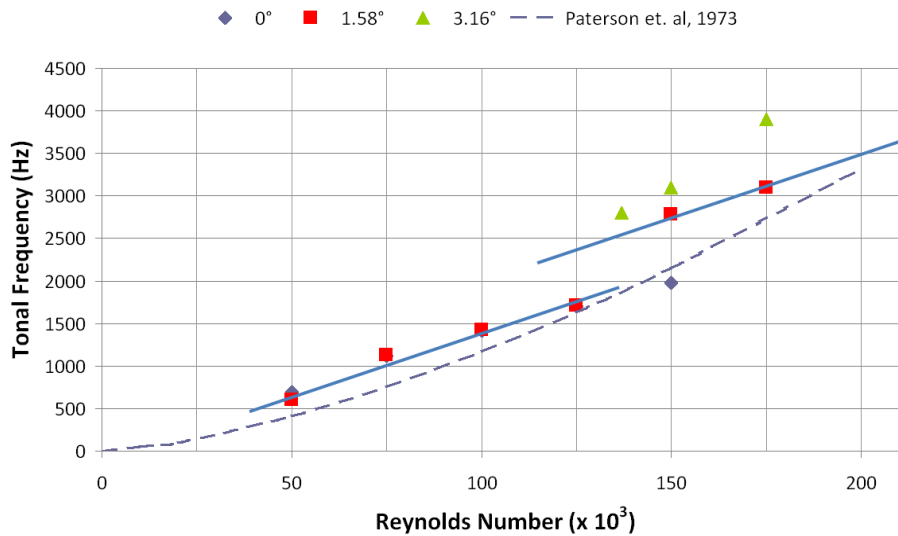


Figure 20: NACA0012 Airfoil Tonal Frequency "Ladder Structure".

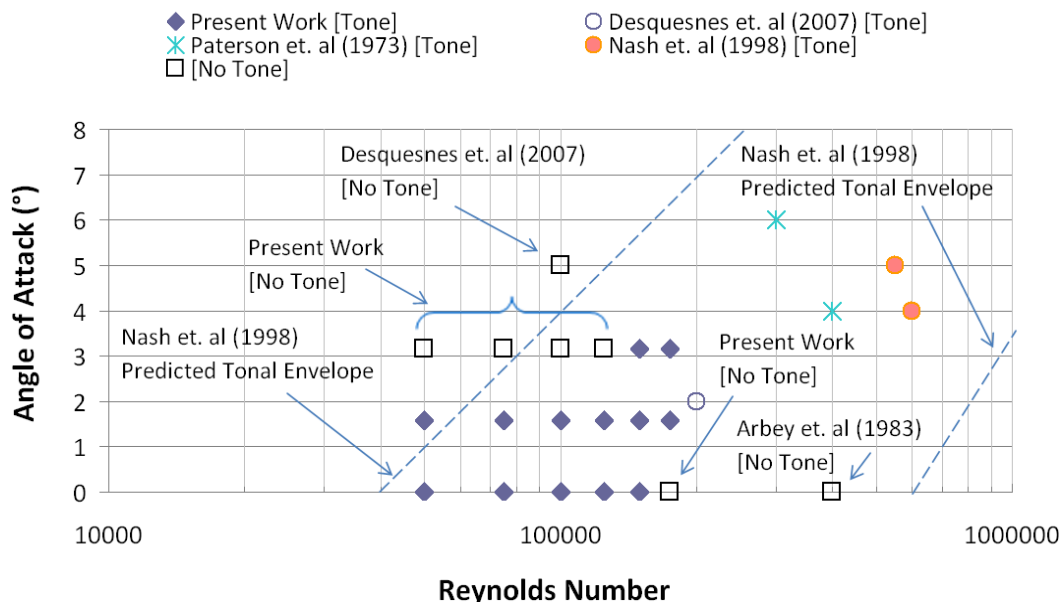


Figure 21: NACA0012 Airfoil Measured Tones and No Tones, including a Predicted Tonal Envelope (Nash et al. 1999).

The results presented in this paper closely match those of Arbey et al (1983). In their work it is strongly suggested that the defined noise spectra are due to an aeroacoustic feedback mechanism which takes place in the unstable boundary layer. It is the authors' opinion that there indeed exists a feedback mechanism resulting in the tonal noise (also agreed by Chong and Joseph (2009)), which is to be further investigated by the authors.

CONCLUSION

The experimental testing of a NACA0012 airfoil of chord length 67mm in the AWT produced noise spectra which is typical of low Reynolds number trailing edge noise. Tonal behaviour was observed, superimposed on a broadband noise hump. The data was presented to shed some light on the various explanations for the trailing edge noise mechanism.

While conclusive results regarding the trailing edge noise mechanism cannot be drawn from the results presented in this paper alone, the results support the following:

- A significant angle of attack requires a larger Reynolds number to observe tonal behaviour as compared to $\alpha' = 0^\circ$.
- A greater angle of attack displays tonal behaviour at higher Reynolds numbers as compared to $\alpha' = 0^\circ$.
- The existence of the "ladder structure" (Paterson et al. 1973) at $\alpha' = 1.58^\circ$ for a NACA0012 airfoil.
- NACA0012 airfoils at $\alpha' = 0^\circ$ cease to display tonal behaviour for $Re > 150,000$.
- Noise magnitudes (for frequencies greater than approximately 2.5kHz) increase with increasing Reynolds number for angles of attack up to (but not limited to) 3.16° , for a 67mm chord NACA0012 airfoil.
- Noise magnitudes (for frequencies less than approximately 2.5kHz) for $\alpha' = 0^\circ$ and 1.58° are maximised for $50,000 \leq Re \leq 150,000$, for a 67mm chord NACA0012 airfoil. At $\alpha' = 3.16^\circ$, the noise magnitudes of all measured frequencies increase with increasing Reynolds number.

FUTURE WORK

It is the authors' intention to further pursue this study, via the use of more refined experimental methods, including the use of aeroacoustic beamforming in conjunction with hot-wire anemometry. It is hoped that much deeper insight can be attained into the acoustic feedback mechanism for the trailing edge noise of airfoils at low Reynolds number.

The AWT will be fitted with up to 63 microphones on a planar surface above the testing section, which will acquire pressure data and feed into a beamforming code, which will develop maps of sound sources and help pin-point locations of noise generation. The hot-wire anemometry will help provide the airflow velocity components in the immediate proximity of the trailing edge.

In order to achieve a greater range of Reynolds numbers and ensure that the tonal frequencies from the trailing edge are in a manageable frequency range, other airfoils with both shorter and longer chord lengths will be manufactured and installed in the AWT.

ACKNOWLEDGEMENTS

The authors would like to thank the School of Mechanical Engineering at the University of Adelaide for access and use of the facilities and equipment detailed in this paper.

REFERENCES

- Amiet, R. 1977, *Refraction of Sound by a Shear Layer*, 15th AIAA Aeroacoustic Conference, AIAA 1977-54
- Arbey, H. and Bataille, J. 1983, *Noise generated by airfoil profiles placed in a uniform laminar flow*, Journal of Fluid Mechanics, Vol. 134.
- Brooks, T., Pope D. and Marcolini, M. 1989, *Airfoil Self-Noise and Prediction*, Tech. rep., NASA Reference Publication 1218.
- Chong, T. and Joseph, P. 2009, *An Experimental Study of Tonal Noise Mechanism of Laminar Airfoil*, AIAA Paper 09-3345, 15th AIAA/CEAS Aeroacoustic Conference (30th AIAA Aeroacoustic Conference) 11 – 13 May 2009, Miami, Florida, U.S.A.
- Desquesnes, G., Terracol, M. and Sagaut, P. 2007, *Numerical investigation of the tone noise mechanism over laminar airfoils*, Journal of Fluid Mechanics, Vol. 591, pp. 155-182.
- Kingan., M and Pearse, J. 2009, *Laminar boundary layer instability noise produced by an aerofoil*, Journal of Sound and Vibration, 322 (2009) 808-828.
- Nakano, T., Fujisawa, N. and Lee, S. 2006, *Measurement of tonal-noise characteristics and periodic flow structure around NACA0018 airfoil*, Experiments in Fluids, Vol. 40.
- Nash, E., Lowson, M. and McAlpine, A. 1998, *Boundary-layer instability noise on aerofoils*, Journal of Fluid Mechanics, Vol. 382, pp.27-61.
- Paterson, R., Vogt, P., Fink, M. and Munch, C. 1973, *Vortex Noise of Isolated Airfoils*, J.Aircraft, Vol. 10, No. 5.
- Sandberg, R., Jones, L., Sandham, N. and Joseph, P. 2008, *Direct numerical simulations of tonal noise generated by laminar flow past airfoils*, Journal of Sound and Vibration, 320 (2008) 838-858.
- Tam, C. 1974, *Discrete Tones of isolated airfoils*, The Journal of the Acoustic Society of America, Vol. 55, No.6.
- Wang, M. 1998, *Computation of trailing-edge noise at low Mach number using LES and acoustic analogy*, Center for Turbulence Research Annual Research Briefs.